Communications

Generalization of the Equivalence Between Physical Optics and Aperture Integration for Radiation From Open-Ended Structures

Juan M. Rius and Krzysztof A. Michalski

***Abstract*—The theorem of equivalence between the Kirchhoff aperture integration (AI) and the physical-optics (PO) approach applied to the interior walls of a open-ended waveguide [1] is generalized in this letter to the case of any open-ended structure (OES).**

***Index Terms*—Apertures, physical optics (POs), waveguides, open-ended.**

I. Introduction

In a recent letter [1] Maci *et al.* use equivalence principle concepts [2] to prove the equivalence between the physical optics (PO) and Kirchhoff–Kottler approximations for the radiated field of an open-ended waveguide. The purpose of this letter is to present a more general theorem, of which the theorem of Maci *et al.* is a special case. The new theorem applies to the aperture fields and interior wall currents corresponding to an arbitrary open-ended structure, for which modal fields cannot in general be defined. In addition, some insight is given on the physical meaning of the radiated fields computed by aperture integration (AI) or PO approaches.

II. Demonstration

Consider an open-ended structure (OES) with perfectly electrically conducting (PEC) walls, as illustrated in Fig. 1(a). The OES, which may be of finite or semi-infinite extent, is excited by impressed electric and magnetic currents, $\underline{J}^i$ and $\underline{M}^i$, respectively. The resulting electric and magnetic fields are denoted by $\underline{E}$ and $\underline{H}$, respectively. For later reference, the exterior and interior surfaces of the OES walls are denoted by S^{ex} and S^{in}, respectively and the mathematical surface covering the OES aperture by S^a. Furthermore, the exterior and interior regions are denoted by V^{ex} and V^{in}, respectively.

According to the equivalence principle [2], the field ($\underline{E}$, $\underline{H}$) in V^{ex} may be found from the problem shown in Fig. 1(b), where the surface currents are given as

$$\underline{J}_s^{ex} = \hat{\underline{n}} \times \underline{H} \quad \text{on } S^{ex} \tag{1}$$

$$\underline{J}_s^{a} = \hat{\underline{n}} \times \underline{H} \quad \text{on } S^{a} \tag{2}$$

$$\underline{M}_s^{a} = -\hat{\underline{n}} \times \underline{E} \quad \text{on } S^{a} \tag{3}$$

in which $\hat{\underline{n}}$ is a unit surface normal vector directed into V^{ex}. If the fields radiated by $\underline{J}_s^{ex}$ and ($\underline{J}_s^a$, $\underline{M}_s^a$) are denoted by ($\underline{E}^{ex}$, $\underline{H}^{ex}$) and ($\underline{E}^a$, $\underline{H}^a$), respectively, then

$$(\underline{E}^a + \underline{E}^{ex}, \underline{H}^a + \underline{H}^{ex}) = \begin{cases} (\underline{E}, \underline{H}) & \text{in } V^{ex} \\ (\underline{0}, \underline{0}) & \text{in } V^{in}. \end{cases} \tag{4}$$

The field ($\underline{E}$, $\underline{H}$) in V^{in} may be found from the equivalent problem shown in Fig. 1(c) [2], where $\underline{J}_s^a$ and $\underline{M}_s^a$ are given by (2) and (3), respectively, and

$$\underline{J}_s^{in} = \hat{\underline{n}} \times \underline{H} \quad \text{on } S^{in} \tag{5}$$

in which $\hat{\underline{n}}$ points into V^{in}. If the fields radiated by $\underline{J}_s^{in}$ and ($\underline{J}^i$, $\underline{M}^i$) are denoted by ($\underline{E}^{in}$, $\underline{H}^{in}$) and ($\underline{E}^i$, $\underline{H}^i$), respectively, then

$$\left(\underline{E}^i + \underline{E}^{in} - \underline{E}^a, \underline{H}^i + \underline{H}^{in} - \underline{H}^a\right) = \begin{cases} (\underline{0}, \underline{0}) & \text{in } V^{ex} \\ (\underline{E}, \underline{H}) & \text{in } V^{in} \end{cases} \tag{6}$$

or, equivalently,

$$\left(\underline{E}^i + \underline{E}^{in}, \underline{H}^i + \underline{H}^{in}\right) = \begin{cases} (\underline{E}^a, \underline{H}^a) & \text{in } V^{ex} \\ (\underline{E} + \underline{E}^a, \underline{H} + \underline{H}^a) & \text{in } V^{in} \end{cases} \tag{7}$$

which leads to the conclusion that the field in V^{ex} due to the aperture currents ($\underline{J}_s^a$, $\underline{M}_s^a$) is equal to the field due to the currents in the interior of the OES, namely the induced current $\underline{J}_s^{in}$ and the impressed currents ($\underline{J}^i$, $\underline{M}^i$).

Note that the currents of the external and internal equivalent problems radiate in the absence of the OES. Hence, the "impressed field" ($\underline{E}^i$, $\underline{H}^i$) should not be confused with the modal-incident field, which satisfies the boundary conditions at the OES walls.

An important observation regarding (7) is that this relationship holds even if there are material objects present outside the OES of Fig. 1(a). Consider, for example, the infinite waveguide of Fig. 1(d), which is obtained by extending the waveguide of Fig. 1(a). Let us denote $S_v = S + S'$ the new virtual surface of Fig. 1(d), which partially superimposes with the actual surface S.

Clearly, the internal equivalent problem of Fig. 1(c) is equally applicable to both the original structure of Fig. 1(a) and its extended version of Fig. 1(d). Hence, the following theorem: the field due to the aperture currents ($\underline{J}_s^a$, $\underline{M}_s^a$) is, in V^{ex}, equal to that radiated by the interior wall current $\underline{J}_s^{in}$ plus the impressed field *irrespective of whether the field* ($\underline{E}$, $\underline{H}$) *used to compute the equivalent currents is derived from the OES (i.e., open-ended waveguide) or the extended structure (i.e., infinite waveguide).* That is, the theorem is valid for any field distribution ($\underline{E}$, $\underline{H}$) that satisfies the wave equation in V^{in} and the boundary conditions in S^{in}. There is an infinity of such field distributions, each satisfying different boundary conditions in V^{ex}.

When ($\underline{E}$, $\underline{H}$) is taken to be a modal field propagating in the extended structure, the equivalent currents are easily determined and the field in V^{ex} may be approximately computed by integrating either $\underline{J}_s^{in}$ or $\underline{J}_s^a$ and $\underline{M}_s^a$ against the free-space Green's functions. Maci *et al.* refer to these two approaches as POs and Kirchhoff–Kottler aperture integration, respectively. Since a modal field is source free, the impressed field ($\underline{E}^i$, $\underline{H}^i$) is absent in (7) and the above theorem specializes to that of Maci *et al.*, which states that the PO and Kirchhoff-Kottler aperture integration are equivalent in V^{ex}. As is evident from (4), both approaches neglect the contribution of the exterior wall current, $\underline{J}_s^{ex}$.

Although arbitrary, the unique virtual surface S_v of Fig. 1(d) which has a practical sense in most cases is that for which the field solution is known in analytical form when S_v has the same boundary conditions of the original surface on S, Fig. 1(a), and arbitrary boundary conditions on S'. The above closed-form solution is usually obtained when the field in S_v is expressed in terms of modes. In this case, the generalization presented in this letter is the same as that suggested in [3] and

Manuscript received August 10, 1998; revised April 7, 2000.

J. M. Rius is with the Department of Signal Theory and Communications, Universitat Politècnica de Catalunya, 08034 Barcelona, Spain.

K. A. Michalski is with the Electromagnetics & Microwave Laboratory, Department of Electrical Engineering, Texas A&M University, College Station, TX 77843-3128 USA.

Publisher Item Identifier S 0018-926X(02)05733-2.

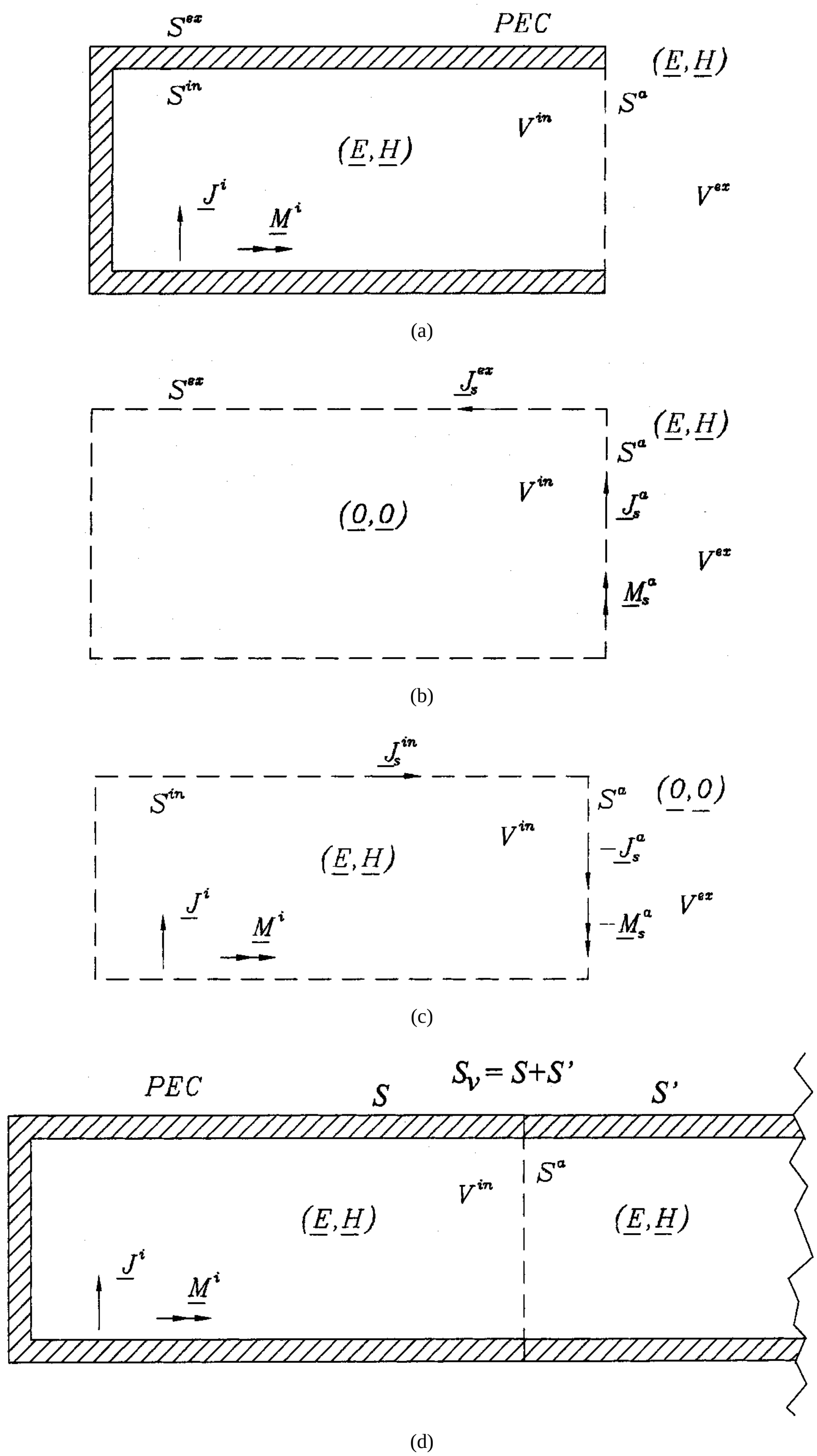

Fig. 1. (a) OES. (b) External equivalent problem. (c) Internal equivalent problem. (d) Extended structure. The virtual surface S_v partially superimposes with the actual surface S.

that can be simply expressed invoking the modal currents in place of the PO currents.

However, the generalized theorem presented in this paper may be a useful tool for field estimation even if a closed-form solution is not available for the field in S_v. If this is the case, one must resort to numerical methods in order to obtain a good approximation of the aperture fields ($\underline{E}^a$, $\underline{H}^a$) and the aperture equivalent currents ($\underline{J}_s^a$, $\underline{M}_s^a$).

To account for the contribution of $\underline{J}_s^{ex}$, one can use an alternative formulation of the equivalence principle [2] and place a PEC wall at S^{ex} in the exterior equivalent problem of Fig. 1(b). Now, in the presence of the PEC wall that corresponds to the original OES, $\underline{J}_s^{ex}$ does not radiate and ($\underline{J}_s^a$, $\underline{M}_s^a$) radiate the original field ($\underline{E}$, $\underline{H}$). To approximately compute the radiation of ($\underline{J}_s^a$, $\underline{M}_s^a$) in the presence of the OES, reflections at surfaces and diffraction at edges may be taken into account by using high-frequency techniques [4], thus leading to a better approximation than ($\underline{E}^a$, $\underline{H}^a$)—the free-space field of ($\underline{J}_s^a$, $\underline{M}_s^a$). Now, the equivalence between the interior-wall currents and the aperture currents becomes approximate; the accuracy of one approximation with respect to the other cannot be stated *a priori* and must be checked case by case.

ACKNOWLEDGMENT

The authors would like to thank the reviewers for their suggestions to improve the clarity of the presentation.

REFERENCES

[1] S. Maci, P. Ya. Ufimtsev, and R. Tiberio, "Equivalence between physical optics and aperture integration for radiation from open ended waveguides," *IEEE Trans. Antennas Propagat.*, vol. 45, pp. 183–185, Jan. 1997.

[2] R. F. Harrington, *Time-Harmonic Electromagnetic Fields*. New York: MacGraw-Hill, 1961, ch. 3, sec. 3–5.

[3] S. Maci, P. Ya. Ufimtsev, and R. Tiberio, "Equivalence between physical optics and aperture integration for antennas and scattering problems," in Proc. URSI Symp. Montreal, July 13–18, 1997.

[4] A. K. Battacharyya, *High-Frequency Electromagnetic Techniques*. New York: Wiley, 1995.

Design and Scan Performance of Large, Probe-Fed Stacked Microstrip Patch Arrays

R. B. Waterhouse

***Abstract*—A strategy is presented on how to design large, direct-contact microstrip patch arrays with broad bandwidths and useful scanning ranges. It will be shown that to maximize these characteristics the lower layer of a stacked patch configuration must have a relatively high dielectric constant, greater than 10 and the upper laminate must have a low dielectric constant value. Doing so yields bandwidths in excess of 25% over a scanning range of $\pm 45^\circ$ in the principle planes. Such arrays may be suitable for millimeter-wave systems such as collision avoidance radars and microcellular mobile communication base stations.**

***Index Terms*—Antenna array feeds, microstrip arrays, stacked microstrip antennas.**

I. INTRODUCTION

Large, unobtrusive, and scannable/multibeam arrays are needed for many applications, including smart antennas for mobile communication base stations and space-borne communication satellites. For these systems narrow beamwidths are required over a reasonable frequency band (typically 20% of the center frequency). Due to its low production cost, low profile and ease of obtaining good polarization purity, the microstrip patch would appear to be an ideal element for the above mentioned array applications. However, in its conventional form, this antenna is typically narrow band and also has limited scanning potential in large arrays due to the excitation of surface waves. These trapped waves cause potential scan blindnesses, limiting the coverage area of the scannable array [1].

Several investigations have been conducted on the scanning performance of microstrip patch arrays and also means of yielding moderate impedance bandwidths over a useful scanning range (for example, [2]). However, relatively large bandwidth/reasonably scannable configurations have yet to be developed. Design strategies have recently been presented for several variations of individual probe-fed microstrip patches resulting in broad bandwidths (greater than 25% [3]). These stacked patch configurations have the potential to satisfy the requirements for the applications given earlier, however their performance in large arrays and their scanning abilities have yet to be investigated. It has also been shown that by simply parasitically coupling a microstrip patch fabricated on a low dielectric constant laminate to a driven patch etched on a high dielectric constant material can result in a broadband, highly efficient antenna [4]. Such a configuration would allow for the simple integration of the antenna directly with photonic and microwave devices and circuits, minimizing the number of layers or material transitions and interconnects required for the transceiver units. Once again, the performance of such a microstrip antenna in a large array environment has yet to be investigated.

In this paper, a thorough, theoretical investigation of the impedance behavior and scanning potential of probe-fed microstrip patch arrays consisting of broad-band stacked elements will be presented. In particular design methodologies to maximize both the bandwidth and scanning range of these arrays will be given. It will be shown that broad impedance bandwidths over useful scanning ranges can be achieved depending on the choice of dielectric constant for the lower microwave laminate. Importantly, the developed design strategy does not require matching networks to give the resulting bandwidths and therefore yields very simple antenna structures and avoids potential blindnesses associated with these networks [2]. All the arrays examined were analyzed using a full-wave spectral domain infinite array analysis.

II. THEORY AND CONFIGURATION

Fig. 1 shows the unit cell of the probe-fed stacked patch array. Here a rectangular stacked patch element is fed by a coaxial pin located at (ρ_p, ϕ_p) from the center of the bottom patch. The lower patch resides on a grounded dielectric layer with a dielectric constant of ε_{r1}, a loss tangent, $\tan\delta_1$ and a thickness d_1. The parasitic coupled patch is mounted on a laminate with a dielectric constant ε_{r2}, a loss tangent, $\tan\delta_2$ and a thickness d_2. The unit cell size is a in the x-direction and b in the y-direction for the array. To investigate the performance of the probe-fed stacked patch configuration, the full-wave analysis presented in [5] was used (refer to [5] for details and experimental verification). It should be noted that although *hi–lo* configurations would typically incorporate edge feeding of the driven element, it has been shown that edge and probe feeding these structures give similar responses [4]. Therefore, for the ease of analysis, only probe-fed configurations are presented here.

III. PROBE-FED STACKED PATCH ARRAYS

An infinite array of probe fed rectangular stacked patches at broadside ($\theta = 0^\circ$) was designed. Here $\varepsilon_{r1} = 2.2$, $d_1 = 0.02\lambda_c$ and $\varepsilon_{r2} = 1.07$ and $d_2 = 0.025\lambda_c$, where λ_c is the center frequency of the band of interest. The 10 dB return loss bandwidth of the antenna was approximately 27% and the response resembled that for a single stacked patch (approximately 30%) using this combination of dielectric materials [3]. The design procedure is in fact fairly similar to [3] in terms of dielectric constant selection; starting points for the conductor

Manuscript received October 19, 1999; revised June 15, 2001.

The author is with the School of Electrical and Computer Systems Engineering, RMIT University, Melbourne VIC 3001, Australia (e-mail: r.waterhouse@ieee.org).

Publisher Item Identifier S 0018-926X(02)05740-X.